Transverse Normal Stress Effects in Multilayered Plates

E. Carrera
Research Professor,
Department of Aerospace Engineering,
Politecnico di Torino,
Corso Duca degli Abrussi 24,
10129 Torino, Italy
e-mail: carrera@polito.it

An evaluation of transverse normal stress σ_{zz} effects in multilayered plate modeling is given in this paper. Mixed theories with continuous interlaminar transverse shear and normal stresses have been formulated on the basis of Reissner's theorem (Reissner, 1984). The case in which the number of the displacement variables preserves independence by the number of constitutive layers, N_l, has been investigated. Classical models based on standard displacement formulations have been discussed for comparison purposes. The analysis of transverse stress effects has been conducted by allowing a constant, linear, and higher-order distribution of the transverse displacement components in the plate thickness directions. Related two-dimensional models are compared for the static response of symmetrically and unsymmetrically layered, simply supported plates made of isotropic as well as orthotropic layers. The conducted numerical investigation and comparison with available results have above all led to the following conclusions. The possibility of including σ_{zz} makes the used mixed theories more attractive that other available modelings. σ_{zz} plays a fundamental role in thick laminate plates analysis. Such a role increases in transversely anisotropic multilayered plate analysis. With an increase of the plate thickness, a very accurate description of σ_{zz} requires modelings whose number of independent variables depends on N_l.

1 Introduction

Elasticity solutions on layered plates (Pagano, 1969; Noor and Burton, 1989) and shells (Ren, 1987; Varadan and Bhaskar, 1991) indicate a number of requirements to accurately describe their elastodynamic response. Among these, the fulfillment of interlaminar continuity of the transverse stresses (shear and normal components), as well as the so-called zigzag form of the displacement field in the thickness direction, are necessary requirements. Very accurate analyses which consider each layer individually *layer-wise models* (LWM) (or multilayers or individual single-layer models) have confirmed these conclusions for the static (Srinivas, 1973; Mau, 1973; Toledano and Murakami, 1987a; Robbins and Reddy, 1993; Carrera, 1998a) and dynamic (Cheung and Wu, 1972; Barbero, Reddy, and Teply, 1990; Cho, Bert, and Striz, 1991; Carrera, 1998b, c) analysis of plate and shell structures. Herein attention is focused on the so-called *equivalent single-layer models* (ESLM). In such a case the number of resulting variables is independent of the number of N_l layers. The work by Hildebrand, Reissner, and Thomas (1940) and by Lo, Christensen, and Wu (1977) are examples of analyses in which higher-order displacement models have been employed. An interesting survey on this subject has been given by Reissner (1985). More recent studies on so-called p-extension, which are mainly oriented to finite element applications, have been probed by Szabo and Sahrmann (1988) and Surana and Sorem (1991). These types of classical theories do not include interlaminar continuity for the transverse shear and normal stresses nor allow the zigzag form for the displacement variables. The intrinsic coupling experienced by orthotropic material between in-plane σ_{xx}, σ_{yy} and out-of-plane σ_{zz} stresses makes the a priori fulfillment of σ_{zz} interlaminar equilibria diffult. Transverse normal stress has, in fact, been discarded in most of the available ESLM analyses. Interlaminar equilibria is usually restricted to the transverse shear components while the zigzag form appears only in the two in-plane components of the displacement. Among these analyses one can mention the early works by Ambartsumian (1968), Whitney (1969), and Rath and Das (1973), which have been more recently revised and extended by Bhashar and Varadan (1989), Di Sciuva (1993), Cho and Parmerter (1993), Soldatos and Timarci (1993), and Idlbi, Karama, and Touratier (1997). A different approach was introduced by Ren (1986) who extended an early theory by Lekhnitskii (1935) to plates that had been presented for beams; the resulting model showed the same restrictions as the previously mentioned analyses. To overcome these restrictions, Reissner proposed a mixed variational theorem RMVT which permits one to assume two independent interlaminar continuous fields for the displacements and transverse stresses (including σ_{zz} components). Similar conclusions were achieved as can be seen in Russian literature (see the very interesting and exhaustive overview presented by Grigolyuk and Kulikov (1988)). A complete discussion on the use of RMVT has recently been presented by the Author (Carrera, 1995, 1997). As far as ESLM is concerned, RMVT was employed by Murakami (1986) and Toledano and Murakami (1987b). σ_{zz} was discarded by Murakami (1986) but retained by Toledano and Murakami (1987b). Extensions to the shells of Murakami's theory were developed by Bhaskar and Varadan (1992) and Jing and Tzeng (1993).

To the best of the author's knowledge there is no available study in which the effects of normal stress σ_{zz} (both interlaminar continuity and zigzag form of transverse displacement u_z) are considered in the framework of ESL analyses. Such a study could establish the limitations of those modelings in which the σ_{zz} stress is neglected. The focus of the current work is directed towards removing this lack.

It would appear clear from the above-mentioned literature that such an aim could be reached in the framework of Reissner's mixed theorem applications. RMVT is therefore applied in the present work. Attention has herein been restricted to plate geometries. The classical model based on the standard displacement formulation is also derived. An analysis of transverse stress effects has been conducted by allowing different polynomials order N in the assumed expansions of displacement and/or stress unknowns. A layer-wise model which has been shown (Carrera, 1998a, b, c) to give a quasi-three-dimensional description of multilayered

Contributed by the Applied Mechanics Division of The American Society of Mechanical Engineers for publication in the ASME Journal of Applied Mechanics.
Discussion on the paper should be addressed to the Technical Editor, Professor Lewis T. Wheeler, Department of Mechanical Engineering, University of Houston, Houston, TX 77204-4792, and will be accepted until four months after final publication of the paper itself in the ASME Journal of Applied Mechanics.
Manuscript received by the ASME Applied Mechanics Division, July 24, 1998; final revision, Mar. 5, 1999. Associate Technical Editor: W. K. Liu.

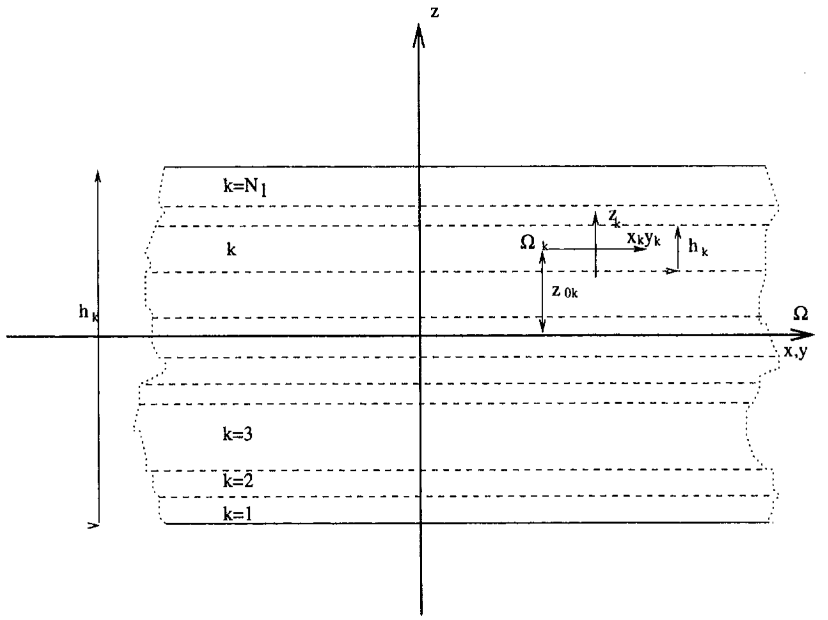

Fig. 1 Multilayered plate

structures is also introduced. This model has herein been used as a reference solution to assess simplified ESL analyses. All these models in this paper are written in a unified manner by referring to techniques developed by the author in earlier works.

2 Preliminary

The geometry and coordinate system of the laminated plates of N_l layers are shown in Fig. 1. The integer k, which is extensively used as both subscripts or superscripts, denotes the layer number that starts from the plate bottom. x and y are the plate middle surface Ω^k coordinates. Γ^k is the layer boundary on Ω^k. z and z_k are the plate and layer thickness coordinates; h and h_k denote the plate and layer thickness, respectively. $\zeta_k = 2z_k/h_k$ is the nondimensioned local plate coordinate; A_k denotes the k-layer thickness domain. Symbols that are not affected by the k subscript/superscripts refer to the whole plate.

The lamina are considered to be homogeneous and to operate in the linear elastic range. Stiffness coefficients are employed in standard form of the Hooke's law for the anisotropic k-lamina. This reads $\sigma_i = \tilde{C}_{ij}\epsilon_j$ where the subindices i and j, ranging from 1 to 6, stand for the index couples 11, 22, 33, 13, 23, and 12, respectively. The material is assumed to be orthotropic as specified by $\tilde{C}_{14} = \tilde{C}_{24} = \tilde{C}_{34} = \tilde{C}_{64} = \tilde{C}_{15} = \tilde{C}_{25} = \tilde{C}_{35} = \tilde{C}_{65} = 0$. This implies that σ^k_{xz} and σ^k_{yz} depend only on ϵ^k_{xz} and ϵ^k_{yz}. In matrix form

$$\boldsymbol{\sigma}^k_{pH_d} = \tilde{\mathbf{C}}^k_{pp}\boldsymbol{\epsilon}^k_{pG} + \tilde{\mathbf{C}}^k_{pn}\boldsymbol{\epsilon}^k_{nG}$$

$$\boldsymbol{\sigma}^k_{nH} = \tilde{\mathbf{C}}^k_{np}\boldsymbol{\epsilon}^k_{pG} + \tilde{\mathbf{C}}^k_{nn}\boldsymbol{\epsilon}^k_{nG} \tag{1}$$

where

$$\tilde{\mathbf{C}}^k_{pp} = \begin{bmatrix} \tilde{C}^k_{11} & \tilde{C}^k_{12} & \tilde{C}^k_{16} \\ \tilde{C}^k_{12} & \tilde{C}^k_{22} & \tilde{C}^k_{26} \\ \tilde{C}^k_{16} & \tilde{C}^k_{26} & \tilde{C}^k_{66} \end{bmatrix}, \quad \tilde{\mathbf{C}}^k_{pn} = \tilde{\mathbf{C}}^{k^T}_{np} = \begin{bmatrix} 0 & 0 & \tilde{C}^k_{13} \\ 0 & 0 & \tilde{C}^k_{23} \\ 0 & 0 & \tilde{C}^k_{36} \end{bmatrix},$$

$$\tilde{\mathbf{C}}^k_{nn} = \begin{bmatrix} \tilde{C}^k_{44} & \tilde{C}^k_{45} & 0 \\ \tilde{C}^k_{45} & \tilde{C}^k_{55} & 0 \\ 0 & 0 & \tilde{C}^k_{66} \end{bmatrix}.$$

Boldface letters denote arrays. The superscript T signifies array transposition. The subscripts n and p denote transverse (out-of-plane, normal) and in-plane values, respectively. Therefore

$$\boldsymbol{\sigma}^k_p = \{\sigma^k_{xx}, \sigma^k_{yy}, \sigma^k_{xy}\}, \quad \boldsymbol{\sigma}^k_n = \{\sigma^k_{xz}, \sigma^k_{yz}, \sigma^k_{zz}\}$$

$$\boldsymbol{\epsilon}^k_p = \{\epsilon^k_{xx}, \epsilon^k_{yy}, \epsilon^k_{xy}\}, \quad \boldsymbol{\epsilon}^k_n = \{\epsilon^k_{xz}, \epsilon^k_{yz}, \epsilon^k_{zz}\}.$$

It should be noticed that σ_{zz} couples the in-plane and out-of-plane stress and strain components. Subscript H denotes stresses evaluated with Hooke's law while subscript G denotes the strain from the geometrical relation Eq. (3). Further subscript d signifies values employed in the displacement formulation. Equation (1) is used in conjunction with a standard displacement formulation, while, for the adopted mixed solution procedure, the stress-strain relationships are conveniently put in the following mixed form:

$$\boldsymbol{\sigma}^k_{pH} = \mathbf{C}^k_{pp}\boldsymbol{\epsilon}^k_{pG} + \mathbf{C}^k_{pn}\boldsymbol{\sigma}^k_{nM}$$

$$\boldsymbol{\epsilon}^k_{nH} = \mathbf{C}^k_{np}\boldsymbol{\epsilon}^k_{pG} + \mathbf{C}^k_{nn}\boldsymbol{\sigma}^k_{nM} \tag{2}$$

where both stiffness and compliance coefficients are employed. The subscript M states that the transverse stresses are those of the assumed model in Eq. (14) (see the next sections). The relation between the arrays of coefficients in the two forms of Hooke's law is simply found:

$$\mathbf{C}^k_{pp} = \tilde{\mathbf{C}}^k_{pp} - \tilde{\mathbf{C}}^k_{pn}\tilde{\mathbf{C}}^{k^{-1}}_{nn}\tilde{\mathbf{C}}^k_{np}, \quad \mathbf{C}^k_{pn} = \tilde{\mathbf{C}}^k_{pn}\tilde{\mathbf{C}}^{k^{-1}}_{nn}$$

$$\mathbf{C}^k_{np} = -\tilde{\mathbf{C}}^{k^{-1}}_{nn}\tilde{\mathbf{C}}^k_{np}, \quad \mathbf{C}^k_{nn} = \tilde{\mathbf{C}}^{k^{-1}}_{nn}.$$

Superscript -1 denotes an inversion of the array.

The strain components $\boldsymbol{\epsilon}^k_p$, $\boldsymbol{\epsilon}^k_n$ are linearly related to the displacements $\mathbf{u}^k(\{u^k_x, u^k_y, u^k_z\})$, according to the following geometrical relations:

$$\boldsymbol{\epsilon}^k_{pG} = \mathbf{D}_p\mathbf{u}^k, \quad \boldsymbol{\epsilon}^k_{nG} = \mathbf{D}_n\mathbf{u}^k. \tag{3}$$

$\mathbf{D}_p$ and $\mathbf{D}_n$ denotes in-plane and out-of-plane differential operators

$$\mathbf{D}_p = \begin{bmatrix} \partial_x & 0 & 0 \\ 0 & \partial_y & 0 \\ \partial_y & \partial_x & 0 \end{bmatrix}; \quad \mathbf{D}_n = \begin{bmatrix} \partial_z & 0 & \partial_x \\ 0 & \partial_z & \partial_y \\ 0 & 0 & \partial_z \end{bmatrix}.$$

3 Displacement and Stress Assumption

3.1 Classical Models. First, classical models are considered. As usual, the displacement variables are expressed in Taylor series

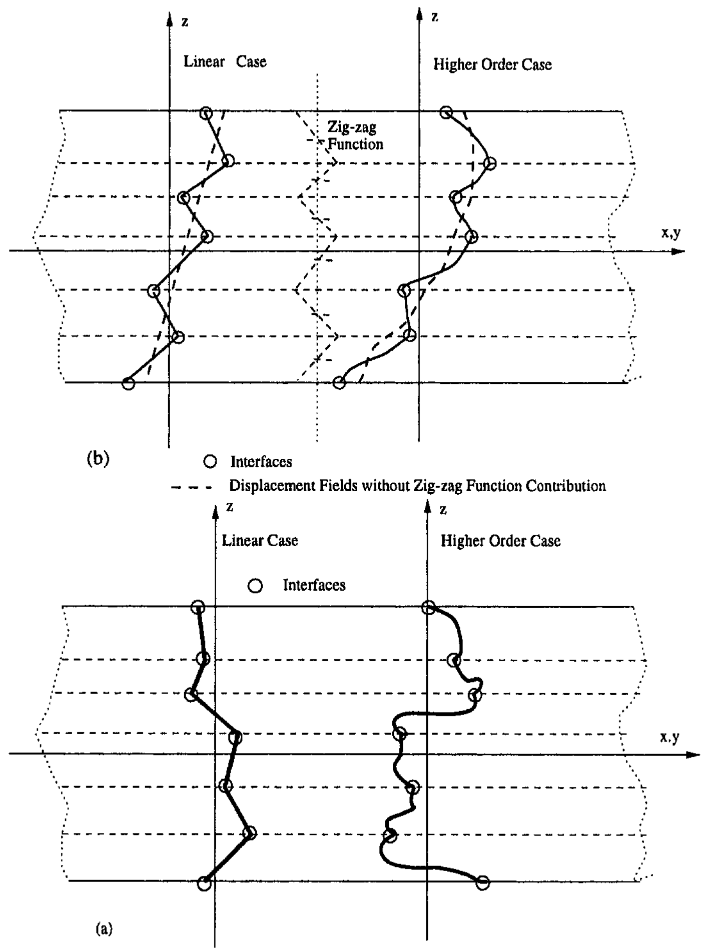

Fig. 2 Displacement and stress fields assumed for the employed models

in terms of unknown variables which are defined on the plate reference surface Ω,

$$\mathbf{u} = \mathbf{u}_0 + z^r \mathbf{u}_r, \quad r = 1, 2, \ldots, N. \tag{4}$$

N is a free parameter of the model. Different values for different modelings and different displacement and stress components are assumed. The repeated r indexes are summed over their ranges. Subscript 0 denotes displacement values with correspondence to the plate reference surface Ω. Linear and higher-order distributions in the z-direction are introduced by the r-polynomials. The assumed models can be written with the same notations that will be adopted for the layer-wise stress model Eq. (9). Equation (4) is therefore rewritten

$$\mathbf{u} = F_t \mathbf{u}_t + F_b \mathbf{u}_b + F_r \mathbf{u}_r = F_\tau \mathbf{u}_\tau,$$
$$\tau = t, b, r, \quad r = 1, 2, \ldots, N-1. \tag{5}$$

Subscript b denotes values related to the plate reference surface $\Omega(\mathbf{u}_b = \mathbf{u}_0)$ while subscript t refers to the highest term $(\mathbf{u}_t = \mathbf{u}_N)$. The F_τ functions assume the following explicit form

$$F_b = 1, \quad F_t = z^N, \quad F_r = z^r, \quad r = 1, 2, \ldots, N-1. \tag{6}$$

Transverse stress σ_{zz} and strain ϵ_{zz} effects are discarded by forcing a constant $(N = 0)$ distribution for the u_z-expansion.

3.2 Mixed Models. The zigzag form of the displacement fields can be reproduced in Eq. (4) by employing the Murakami idea (Murakami, 1986). In the framework of the ESL description and according to Murakami (1986), a zigzag term can be introduced into Eq. (4) (see Fig. 2):

$$\mathbf{u}^k = \mathbf{u}_0 + (-1)^k \zeta_k \mathbf{u}_Z + z^r \mathbf{u}_r, \quad r = 1, 2, \ldots, N. \tag{7}$$

Subscript Z refers to the introduced zigzag term. With unified notations Eq. (8) becomes

$$\mathbf{u}^k = F_t \mathbf{u}_t + F_b \mathbf{u}_b + F_r \mathbf{u}_r = F_\tau \mathbf{u}_\tau,$$
$$\tau = t, b, r, \quad r = 1, 2, \ldots, N. \tag{8}$$

Subscript t refers to the introduced zigzag term $(\mathbf{u}_t = \mathbf{u}_Z,\ F_t = (-1)^k \zeta_k)$. The F_t functions assume the following explicit form. It should be noticed that F_t assumes the values ± 1 in correspondence to the bottom and the top interface of the k-layer (see Fig. 2).

The thickness expansion used for displacement variables in Eq. (8) is not suitable for the transverse stress cases. For instance, homogeneous top-bottom plate surface conditions cannot be imposed. Transverse stresses are therefore herein described by means of the layer-wise description (Murakami, 1986; Toledano-Murakami, 1987b; Carrera, 1995, 1998a)

$$\boldsymbol{\sigma}^k_{nM} = F_t \boldsymbol{\sigma}^k_{nt} + F_b \boldsymbol{\sigma}^k_{nb} + F_r \boldsymbol{\sigma}^k_{nr} = F_\tau \boldsymbol{\sigma}^k_{n\tau}, \quad \tau = t, b, r,$$
$$r = 2, 3, \ldots, N; \quad k = 1, 2, \ldots, N_l. \tag{9}$$

In contrast to in Eq. (8), it is now intended that the subscripts t and b denote values related to the layer top and bottom surface, respectively. They consist of the linear part of the expansion. The thickness functions $F_\tau(\zeta_k)$ have now been defined at the k-layer level,

$$F_t = \frac{P_0 + P_1}{2}, \quad F_b = \frac{P_0 - P_1}{2},$$

$$F_r = P_r - P_{r-2}, \quad r = 2, 3, \ldots, N, \tag{10}$$

in which $P_j = P_j(\zeta_k)$ is the Legendre polynomial of the j-order defined in the ζ_k-domain: $-1 \le \zeta_k \le 1$. The parabolic, cubic, and fourth-order stress field Eq. (9) will be associated to linear, parabolic, and cubic displacement field Eq. (8), respectively, in the numerical investigations. The related polynomials are

$$P_0 = 1, \quad P_1 = \zeta_k, \quad P_2 = (3\zeta_k^2 - 1)/2,$$

$$P_3 = \frac{5\zeta_k^3}{2} - \frac{3\zeta_k}{2}, \quad P_4 = \frac{35\zeta_k^4}{8} - \frac{15\zeta_k^2}{4} + \frac{3}{8}.$$

The chosen functions have the following properties:

$$\zeta_k = \begin{cases} 1: & F_t = 1; \quad F_b = 0; \quad F_r = 0 \\ -1: & F_t = 0; \quad F_b = 1; \quad F_r = 0. \end{cases} \tag{11}$$

The top and bottom values have been used as unknown variables. The interlaminar transverse shear and normal stress continuity can therefore be easily linked:

$$\boldsymbol{\sigma}_{nt}^k = \boldsymbol{\sigma}_{nb}^{(k+1)}, \quad k = 1, \quad N_l - 1. \tag{12}$$

In those cases in which the top/bottom-shell stress values are prescribed (zero or imposed values), the following additional equilibrium conditions must be accounted for,

$$\boldsymbol{\sigma}_{nb}^1 = \bar{\boldsymbol{\sigma}}_{nb}, \quad \boldsymbol{\sigma}_{nt}^{N_l} = \bar{\boldsymbol{\sigma}}_{nt}, \tag{13}$$

where the overbar is the imposed values in correspondence to the plate boundary surfaces. Examples of linear and higher-order fields have been plotted in Fig. 2. The stress variables could be eliminated by employing the *weak form of Hooke's law* proposed in (Carrera, 1996).

3.3 Layer-Wise Mixed Model. According to Carrera (1995, 1998a) two independent layer-wise fields are assumed for both displacement and stress variables as in Eq. (9),

$$\begin{aligned} \mathbf{u}^k &= F_t\mathbf{u}_t^k + F_b\mathbf{u}_b^k + F_r\mathbf{u}_r^k = F_\tau\mathbf{u}_\tau^k & \tau &= t, b, r \\ & & r &= 2, 3, \ldots, N \\ \boldsymbol{\sigma}_{nM}^k &= F_t\boldsymbol{\sigma}_{nt}^k + F_b\boldsymbol{\sigma}_{nb}^k + F_r\boldsymbol{\sigma}_{nr}^k = F_\tau\boldsymbol{\sigma}_{n\tau}^k & k &= 1, 2, \ldots, N_l. \end{aligned} \tag{14}$$

In addition to Eq. (12) the compatibility of the displacement reads

$$\mathbf{u}_t^k = \mathbf{u}_b^{(k+1)}, \quad k = 1, \quad N_l - 1. \tag{15}$$

4 Governing Equations

In order to write all the models mentioned in the previous section it is convenient to refer to all the stress and displacement variables at the k-layer level, i.e., to use a layer-wise description. ESL cases are achieved by writing the governing equations at the multilayered plate level.

The displacement approach is formulated in terms of $\mathbf{u}^k$ by variatianally imposing the equilibrium via the principle of virtual displacements. In the static case this establishes

$$\sum_{k=1}^{N_l} \int_{\Omega^k} \int_{A_k} (\delta\boldsymbol{\epsilon}_{pG}^{k^T}\boldsymbol{\sigma}_{pH_d}^k + \delta\boldsymbol{\epsilon}_{nG}^{k^T}\boldsymbol{\sigma}_{nH_d}^k) d\Omega^k dz = \delta L^e \tag{16}$$

where δ signifies virtual variations. The variation of the internal work has been split into in-plane and out-of-plane parts and involves the stress obtained from Hooke's Law and the strain from the geometrical relations. δL_e is the virtual variation of the work done by the external layer-forces $\mathbf{p}^k(\{p_x^k, p_y^k, p_z^k\})$.

In the mixed case, the equilibrium and compatibility are both formulated in terms of the $\mathbf{u}^k$ and $\boldsymbol{\sigma}_n^k$ unknowns via Reissner's mixed variational theorem (Reissner, 1984, 1986),

$$\sum_{k=1}^{N_l} \int_{\Omega^k} \int_{A_k} (\delta\boldsymbol{\epsilon}_{pG}^{k^T}\boldsymbol{\sigma}_{pH}^k + \delta\boldsymbol{\epsilon}_{nG}^{k^T}\boldsymbol{\sigma}_{nM}^k + \delta\boldsymbol{\sigma}_{nM}^{k^T}(\boldsymbol{\epsilon}_{nG}^k - \boldsymbol{\epsilon}_{nH}^k)) d\Omega^k dz = \delta L^e. \tag{17}$$

The L.H.S. includes the variations of the internal work in the plate: the first two terms come from the displacement formulation, they lead to variatianally consistent equilibrium conditions; the third "mixed" term variationally enforces the compatibility of the transverse strains components.

Upon substitution of Eqs. (1), (2), and (3), as well as of the requested assumed model Eqs. (4)–(14) and by integrating by parts, the two previous variational equations lead to governing differential equations. These equations were written in Carrera (1998b) in terms of stress and strain resultants; details on the treatment of the variational equations were also reported in this work. For the sake of conciseness, the governing equations have herein been expressed in terms of the introduced stress and displacement variables.

The displacement formulation yields to the following equilibrium conditions:

$$\delta\mathbf{u}_\tau^k: \quad \mathbf{K}_d^{k\tau s}\mathbf{u}_s^k = \mathbf{p}_\tau^k. \tag{18}$$

The related boundary conditions are

$$\mathbf{u}_\tau^k = \bar{\mathbf{u}}_\tau^k \quad \text{or} \quad \boldsymbol{\Pi}_d^{k\tau s}\mathbf{u}_s^k = \boldsymbol{\Pi}_d^{k\tau s}\bar{\mathbf{u}}_s^k \tag{19}$$

while the mixed case leads to the following set of equilibrium and constitutive equations

$$\begin{aligned} \delta\mathbf{u}_\tau^k: &\quad \mathbf{K}_{uu}^{k\tau s}\mathbf{u}_s^k + \mathbf{K}_{u\sigma}^{k\tau s}\boldsymbol{\sigma}_{ns}^k = \mathbf{p}_\tau^k \\ \delta\boldsymbol{\sigma}_{n\tau}^k: &\quad \mathbf{K}_{\sigma u}^{k\tau s}\mathbf{u}_s^k + \mathbf{K}_{\sigma\sigma}^{k\tau s}\boldsymbol{\sigma}_{ns}^k = 0 \end{aligned} \tag{20}$$

and to the boundary conditions

$$\mathbf{u}_\tau^k = \bar{\mathbf{u}}_\tau^k \quad \text{or} \quad \boldsymbol{\Pi}_u^{k\tau s}\mathbf{u}_s^k + \boldsymbol{\Pi}_\sigma^{k\tau s}\boldsymbol{\sigma}_{ns}^k = \boldsymbol{\Pi}_u^{k\tau s}\bar{\mathbf{u}}_s^k + \boldsymbol{\Pi}_\sigma^{k\tau s}\bar{\boldsymbol{\sigma}}_{ns}^k. \tag{21}$$

The further subscript/superscript $s = t, b, r$ has been introduced in order to distinguish the terms related to the introduced variables from those related to their variations. In explicit form

$$\begin{aligned} \mathbf{K}_d^{k\tau s} = {} & -\mathbf{D}_p^T(\tilde{\mathbf{Z}}_{pp}^{k\tau s}\mathbf{D}_p + \tilde{\mathbf{Z}}_{pn}^{k\tau s}\mathbf{D}_{n\Omega} + \tilde{\mathbf{Z}}_{pn}^{k\tau s_z}\mathbf{D}_{n\Omega}) - \mathbf{D}_{n\Omega}^T(\tilde{\mathbf{Z}}_{np}^{k\tau s}\mathbf{D}_p \\ & + \tilde{\mathbf{Z}}_{nn}^{k\tau s}\mathbf{D}_{n\Omega} + \tilde{\mathbf{Z}}_{nn}^{k\tau s_z}) + \tilde{\mathbf{Z}}_{np}^{k\tau_z s}\mathbf{D}_p + \tilde{\mathbf{Z}}_{nn}^{k\tau_z s}\mathbf{D}_{n\Omega} + \tilde{\mathbf{Z}}_{nn}^{k\tau_z s_z} \\ \boldsymbol{\Pi}_d^{k\tau s} = {} & \mathbf{I}_p^T(\tilde{\mathbf{Z}}_{pp}^{k\tau s}\mathbf{D}_p + \tilde{\mathbf{Z}}_{pn}^{k\tau s}\mathbf{D}_{n\Omega} + \tilde{\mathbf{Z}}_{pn}^{k\tau s_z}\mathbf{D}_{n\Omega}) \\ & + \mathbf{I}_{n\Omega}^T(\tilde{\mathbf{Z}}_{np}^{k\tau s}\mathbf{D}_p + \tilde{\mathbf{Z}}_{nn}^{k\tau s}\mathbf{D}_{n\Omega} + \tilde{\mathbf{Z}}_{nn}^{k\tau s_z}) \end{aligned}$$

$$\mathbf{K}_{uu}^{k\tau s} = -\mathbf{D}_p^T\mathbf{Z}_{pp}^{k\tau s}\mathbf{D}_p \quad \mathbf{K}_{u\sigma}^{k\tau s} = -\mathbf{D}_p^T\mathbf{Z}_{pn}^{k\tau s} + E_{\tau_z s}\mathbf{I} - E_{\tau s}\mathbf{D}_{n\Omega}^T$$

$$\mathbf{K}_{\sigma u}^{k\tau s} = E_{\tau s}\mathbf{D}_{n\Omega} + E_{\tau s_z}\mathbf{I} - \mathbf{Z}_{np}^{k\tau s}\mathbf{D}_p \quad \mathbf{K}_{\sigma\sigma}^{k\tau s} = -\mathbf{Z}_{nn}^{k\tau s}$$

$$\boldsymbol{\Pi}_u^{k\tau s} = \mathbf{I}_p^T\mathbf{Z}_{pp}^{k\tau s}\mathbf{D}_p \quad \boldsymbol{\Pi}_\sigma^{k\tau s} = \mathbf{Z}_{pn}^{k\tau s} + E_{\tau s}\mathbf{I}_{n\Omega}^T \tag{22}$$

where

$$\mathbf{D}_{n\Omega} = \begin{bmatrix} 0 & 0 & \partial_x \\ 0 & 0 & \partial_y \\ 0 & 0 & 0 \end{bmatrix}; \quad \mathbf{I} = \begin{bmatrix} 1 & 0 & 0 \\ 0 & 1 & 0 \\ 0 & 0 & 1 \end{bmatrix};$$

$$\mathbf{I}_p = \begin{bmatrix} 1 & 0 & 0 \\ 0 & 1 & 0 \\ 1 & 1 & 0 \end{bmatrix}; \quad \mathbf{I}_{n\Omega} = \begin{bmatrix} 0 & 0 & 1 \\ 0 & 0 & 1 \\ 0 & 0 & 0 \end{bmatrix}.$$

The integration in the thickness coordinate has been a priori carried out as usual in two-dimensional modelings: The following layer-stiffnesses and integrals have been introduced:

$$(\tilde{\mathbf{Z}}_{pp}^{k\tau s}, \tilde{\mathbf{Z}}_{pn}^{k\tau s}, \tilde{\mathbf{Z}}_{np}^{k\tau s}, \tilde{\mathbf{Z}}_{nn}^{k\tau s}, \mathbf{Z}_{pp}^{k\tau s}, \mathbf{Z}_{pn}^{k\tau s}, \mathbf{Z}_{np}^{k\tau s}, \mathbf{Z}_{nn}^{k\tau s})$$
$$= (\tilde{\mathbf{C}}_{pp}^{k}, \tilde{\mathbf{C}}_{pn}^{k}, \tilde{\mathbf{C}}_{np}^{k}, \tilde{\mathbf{C}}_{nn}^{k}, \mathbf{C}_{pp}^{k}, \mathbf{C}_{pn}^{k}, \mathbf{C}_{np}^{k}, \mathbf{C}_{nn}^{k})E_{\tau s}$$
$$(\tilde{\mathbf{Z}}_{pn}^{k\tau s_z}, \tilde{\mathbf{Z}}_{np}^{k\tau_z s}, \tilde{\mathbf{Z}}_{nn}^{k\tau s_z}, \tilde{\mathbf{Z}}_{nn}^{k\tau_z s}, \tilde{\mathbf{Z}}_{nn}^{k\tau_z s_z})$$
$$= (\tilde{\mathbf{C}}_{pn}^{k}E_{\tau s_z}, \tilde{\mathbf{C}}_{np}^{k}E_{\tau_z s}, \tilde{\mathbf{C}}_{nn}^{k}E_{\tau s_z}, \tilde{\mathbf{C}}_{nn}^{k}E_{\tau_z s}, \tilde{\mathbf{C}}_{nn}^{k}E_{\tau_z s_z})$$
$$(E_{\tau s}^{k}, E_{\tau_z s}, E_{\tau s_z}, E_{\tau_z s_z}^{k})$$
$$= \int_{A_k} (F_\tau F_s, F_{\tau_z} F_s, F_\tau F_{s_z}, F_{\tau_z} F_{s_z}) dz. \quad (23)$$

Explicit forms of the governing equations for each layer can be written by expanding the introduced subscripts and superscripts in the previous arrays as follows:

$$k = 1, 2, \ldots, N_l; \ \tau = t, r, b, \ s = t, r, b, \ (r = 2, \ldots, N).$$

4.1 Assembly From Layer to Multilayered Plate Level. In the previous sections mixed and standard displacement formulations have been written for the N_l independent layers. Multilayered equations can be written according to the usual variational statements: Stiffness and/or compliances related to the same variables are accumulated in this process. Interlaminar continuity conditions are imposed at this stage. Details on this procedure can be found in the already mentioned papers (Carrera, 1995, 1998a). Multilayered arrays are introduced. The equilibrium and boundary conditions for the displacement formulation take on the following form:

$$\mathbf{K}_d \mathbf{u} = \mathbf{p}$$
$$\mathbf{u} = \bar{\mathbf{u}} \quad \text{or} \quad \mathbf{\Pi}_d \mathbf{u} = \mathbf{\Pi}_d \bar{\mathbf{u}} \quad (24)$$

while for the mixed case, one has

$$\mathbf{K}_{uu}\mathbf{u} + \mathbf{K}_{u\sigma}\boldsymbol{\sigma}_n = \mathbf{p} + \mathbf{p}_u^{1N_l}$$
$$\mathbf{K}_{\sigma u}\mathbf{u} + \mathbf{K}_{\sigma\sigma}\boldsymbol{\sigma}_n = \mathbf{p}_\sigma^{1N_l} \quad (25)$$

with boundary conditions

$$\mathbf{u} = \bar{\mathbf{u}} \quad \text{or} \quad \mathbf{\Pi}_u \mathbf{u} + \mathbf{\Pi}_\sigma \boldsymbol{\sigma}_n = \mathbf{\Pi}_u \bar{\mathbf{u}} + \mathbf{\Pi}_\sigma \bar{\boldsymbol{\sigma}}_n. \quad (26)$$

$\mathbf{p}_u^{1N_l}$ and $\mathbf{p}_\sigma^{1N_l}$ are the arrays obtained from the transverse stress values imposed at the top/bottom of the plate.

4.2 Closed-Form Solutions for Cross-Ply Laminated Plates. The boundary value problem governed by Eqs. (24), (25), and (26) in the most general case of geometry, boundary conditions and layouts, could be solved by implementing only approximated solution procedures. The particular case in which the material has the properties $\tilde{C}_{16} = \tilde{C}_{26} = \tilde{C}_{36} = \tilde{C}_{45} = 0$, has here been considered, for which Navier-type closed-form solutions can be found by assuming the following harmonic forms for the applied loadings and unknown variables,

$$(u_{x_\tau}^k, \sigma_{xz_\tau}^k, p_{x_\tau}^k) = \sum_{m,n} (U_x^k, S_{xz_\tau}^k, P_{x_\tau}^k) \cos\frac{m\pi x}{a} \sin\frac{n\pi y}{b}$$
$$(u_{y_\tau}^k, \sigma_{yz_\tau}^k, p_{y_\tau}^k) = \sum_{m,n} (U_y^k, S_{yz_\tau}^k, P_{y_\tau}^k) \sin\frac{m\pi x}{a} \cos\frac{n\pi y}{b}$$
$$(u_{z_\tau}^k, \sigma_{zz_\tau}^k, p_{z_\tau}^k) = \sum_{m,n} (U_z^k, S_{zz_\tau}^k, P_{z_\tau}^k) \sin\frac{m\pi x}{a} \sin\frac{n\pi y}{b}. \quad (27)$$

a and b are the plate lengths in the x and y directions, respectively, while m and n are the correspondent wave numbers. Capital letters in the R.H.S. are correspondent maximum amplitudes. On substitution of Eqn. (27), the governing equations assume the form of a linear system of algebraic equations. This procedure has been coded for the different case theories and results are discussed in the next section.

Table 1 List of the acronyms used to denote plate theories

— Theories from literature	
Exact	Three dimensional solution after Pagano (1969)
C&P1, C&P3	Linear and cubic case after Cho and Parmerter (1993)
D&S1, D&S3	Linear and cubic case after Di Sciuva (1993)
IK&T	Idlbi, Karama and Touratier (1997)
LC&W	Lo, Christiansen and Wu (1977)
T&M1,T&M3	Murakami (1986) and Toledano and Murakami (1987b)
Ren	Ren (1986)
— Present Theories	
D1i,D2i,D3i**	Classical models in Eqns.(4)
D1d,D2d,D3d*	Classical models discarding σ_{zz}
D3Zi	Classical models using Eqns.(8) instead of Eqns.(4)
LW4	Mixed layer-wise model Eqn.(14) relate to N=4
M1i,M2i,M3i	Mixed models in Eqn.(8), Eqn.(9)
M1d,M2d,M3d	Mixed models discarding σ_{zz}
M3ia***	M3i-case discarding zigzag $(-1)^k u_{Z_z}$ term.

* suffixes 1,2,3 denote linear, parabolic and cubic u-fields, respectively, while d signifies that σ_{zz} has been discarded.
** suffix i denotes results including σ_{zz}.
*** suffix a refers to analyses discarding the zigzag terms in u_{Z_z} of Eqn.(8).

5 Results and Discussion

Simply supported plates bent by a transverse bi-sinusoidal distribution of normal pressure $p_{z_t}^{N_l}$ applied to the top surface of the whole plate have been considered. Two loading cases $m = 1$, $n = 0$ (cylindrical bending) and $m = n = 1$ have been considered. Several particular case theories related to different N-orders of the expansion in the introduced displacement and stress fields have been considered. The treated subcases are described in Table 1 where the used acronyms are listed. Through the thickness distribution of in-plane and transverse stress and displacement amplitudes have been analyzed. The following nondimensioned parameters have been introduced:

$$\bar{S}_{xz} = S_{xz}/(p_{z_t}^{N_l} a/h), \quad \bar{S}_{zz} = S_{zz}/p_{z_t}^{N_l},$$
$$\bar{U}_x = U_x E_T/(p_{z_t}^{N_l}(a/h)^3), \quad \bar{U}_z = U_z \times 100 E_T h^3/(p_{z_t}^{N_l} a^4)$$

Thin and thick as well as square and rectangular plate geometries have been analyzed. Cross-ply, symmetrically (N_l = 3, 9) and unsymmetrically (N_l = 4) laminated plates are considered in Tables 2–4 and Figs. 2–8. The mechanical data of the lamina are those used by Pagano (1969): $E_L = 25 \times 10^6$ psi, $E_T = 1 \times 10^6$ psi, $G_{LT} = 0.5 \times 10^6$ psi, $G_{TT} = 0.2 \times 10^6$ psi, $\nu_{LT} = \nu_{TT} = .25$; where, following the usual notation (Reddy, 1997), L signifies

Table 2 Maximum transverse displacement $\bar{U}_z$ (z = 0) of thick plate in cylindrical bending. Comparison of present analyses to exact solutions and to available mixed results.

	a/h=4		a/h=6	
	N_l=3	N_l=4	N_l=3	N_l=4
Exact	2.887	4.181	1.635	2.556
T&M3	2.881	4.105	1.634	2.519
C&P3	-	4.083	-	2.501
T&M1	2.907	3.316	1.636	2.107
C&P1	-	3.316	-	2.107
LC&W	2.687	3.587	1.514	2.242
	Present Analysis			
LW4	2.887	4.181	1.625	2.556
	—σ_{zz} included			
M3i	2.881	4.102	1.634	2.514
M2i	2.831	3.478	1.602	2.195
M1i	2.904	3.300	1.634	2.095
	—σ_{zz} discarded			
M3d	2.898	4.124	1.637	2.516
M2d	2.848	3.488	1.605	2.195
M1d	2.904	3.306	1.634	2.098

Table 3 Influence of thickness ration on $\bar{U}_z$ ($z = 0$) and $\bar{S}_{xz}$ ($z = 0$ unless denoted). Rectangular ($b = 3a$) three-layered plates.

	$\bar{U}_z$			$\bar{S}_{xz}$			
a/h	4	10	20	4	z	10	20
Exact	2.820	.919	.610	.387	-	.420	.434
IK&TC	2.729	.918	.609	.378	-	.441	.451
D&S1	2.717	.881	.599	.366	-	.419	-
D&S3	2.757	.919	.610	.329	-	.420	-
Ren	2.80	.920	-	.317	-	.415	-
	Present Analysis						
LW4	2.821	.919	.610	.387	-.23	.420	.434
	—σ_{zz} *included*						
M3i	2.815	.919	.609	.385	-.23	.420	.434
M3ia	2.815	.919	.609	.388	-.23	.420	.434
M2i	2.767	.906	.606	.393	-.23	.421	.435
M1i	2.839	.915	.606	.399	-.23	.420	.434
D3Zi	2.811	.919	.610	.389	.27	.420	.434
D3i	2.625	.867	.596	.378	-.17	.427	.436
	—σ_{zz} *discarded*						
M3d	2.832	.918	.607	.386	±.27	.420	.434
M2d	2.784	.904	.604	.393	±.23	.421	.435
M1d	2.839	.915	.606	.394	±.23	.420	.434
D3Zd	2.828	.918	.607	.348	±.27	.420	.434
D3d	2.644	.866	.593	.377	0	.427	.436

the fiber direction, T the transverse direction, and ν_{LT} is the major Poisson ratio.

Tables 2 and 3 compare present analysis to available results. A good agreement with the mixed models by Murakami (1986) and Toledano and Murakami (1987b) has been found. The LW4 analysis matches the exact solution with excellent accuracy. Such a result confirms (Carrera, 1998a, b, c) the reliability of layer-wise mixed models to give a three-dimensional description of stress and displacement fields in laminated plates. LW4 analysis has in fact been taken as a reference solutions in Table 4 and Figs. 3–12. The improvements introduced by taking σ_{zz} effects into account are evident for the thick plate cases. Higher-order mixed models lead to the best description. A comparison with the other models of Table 3 (C&P1, C&P3, D&S1, D&S3, IK&T which allow interlaminar continuous transverse shear stresses) reveals that the extension of such a continuity to σ_{zz} permits one to conclude that the M3i-model leads to the best ESL results. These comments are further confirmed by comparing the M3d, M2d, M1d to M3i, M2i, M1i analysis. Nevertheless, D3Zi results show that the classical displacement formulation can be greatly improved by introducing a zigzag functions $(-1)^k \mathbf{u}_z$ into Eq. (4).

Table 4 Influence of thickness ratio on $\bar{U}_z$ ($z = 0$). Same data of Table 2 (three-layer case).

a/h	2.5	5	10	100
LW4	5.963	2.091	.9316	.5140
	—σ_{zz} *included*			
M3i	5.912	2.089	.9180	.5140
M3ia	5.912	2.089	.9180	.5140
M2i	5.876	2.045	.9180	.5140
M1i	6.099	2.094	.9284	.5138
D3Zi	5.874	2.087	.9316	.5116
D3i	5.644	1.935	.8793	.5122
	—σ_{zz} *discarded*			
M3d	6.015	2.096	.9309	.5118
M2d	5.982	2.056	.9172	.5117
M1d	6.099	2.094	.9281	.5118
D3Zd	5.978	2.094	.9308	.5118
D3d	5.755	1.943	.8786	.5112

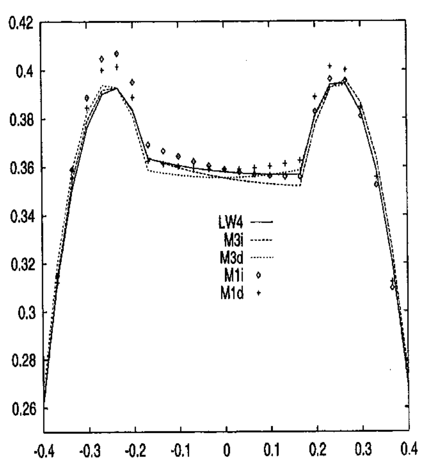

Fig. 3 $\bar{S}_{xz}$ versus z: asymmetry introduced by σ_{zz} effects. Data of Table 2 (three-layers case, $a/h = 4$).

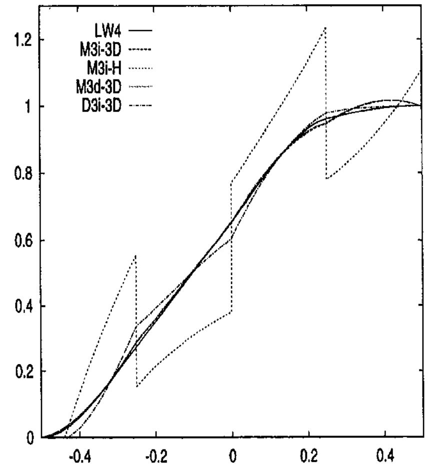

Fig. 4 $\bar{S}_{zz}$ versus z. Data of Table 2 (four-layers case, $a/h = 4$).

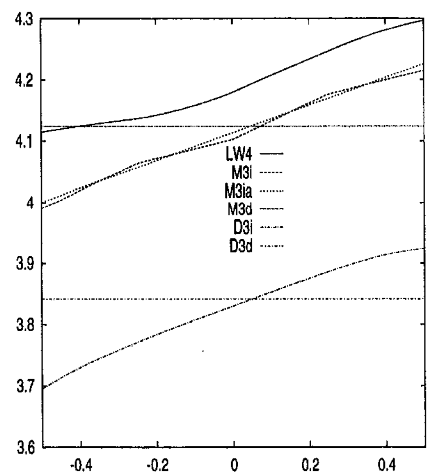

Fig. 5 $\bar{U}_z$ versus z. Data of Table 2 (four-layers case, $a/h = 4$).

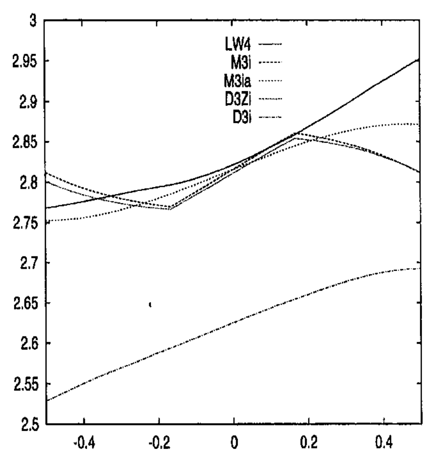

Fig. 6 $\bar{U}_z$ versus z. Data of Table 3 ($a/h = 4$).

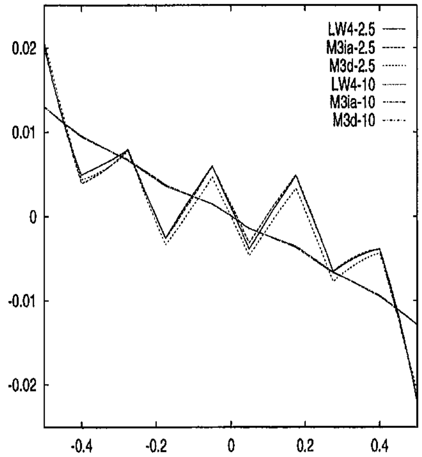

Fig. 7 $\bar{U}_z$ **versus** z**. Data of Table 2 (nine-layers case,** $a/h = 2.5, 10$**).**

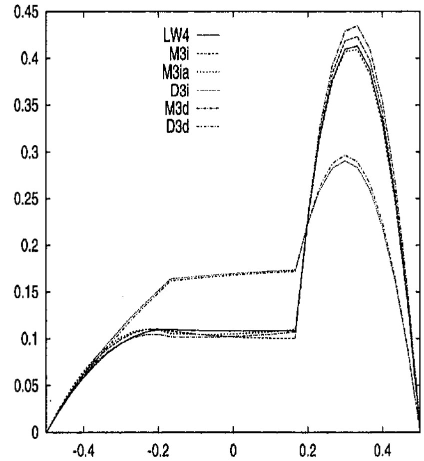

Fig. 10 $\bar{S}_{xz}$ **versus** z**. Square plate made of isotropic layers (Unsymmetrically laminated case,** $a/h = 4$**).**

Figure 3 makes a fundamental limitation of each laminated theory which neglected σ_{zz} evident. The top part of the diagram has been plotted. As confirmed in Table 3 ($a/h = 4$ case) and the plate being loaded at the top surface, σ_{zz} enforces a nonsymmetrical distribution of $\bar{S}_{xz}$ versus z for LW4, M3i, and M1i analyses. On the other hand, M3d and M1d analysis as well as any other plate theories in which σ_{zz} is discarded, cannot improve the transverse stress fields in the whole thickness. The plate being symmetrically laminated, M3d and M1d analyses in fact *tragically* lead to a symmetrical distribution of $\bar{S}_{xz}$ versus z: They cannot, therefore, in any case furnish the nonsymmetrical distribution of the LW4 analysis. Nevertheless, M3i results are very close to LW4 analysis.

Figure 4 shows that Hooke's law (suffix-H) leads to interlaminar discontinuous transverse normal stresses. σ_{zz} is therefore calculated via integration of the three dimensional equilibrium equa-

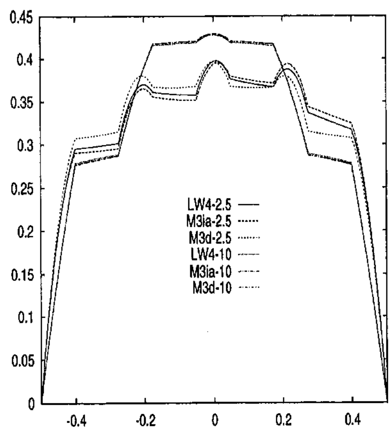

Fig. 8 $\bar{S}_{xz}$ **versus** z**. Data of Table 2 (nine-layers case,** $a/h = 2.5, 100$**).**

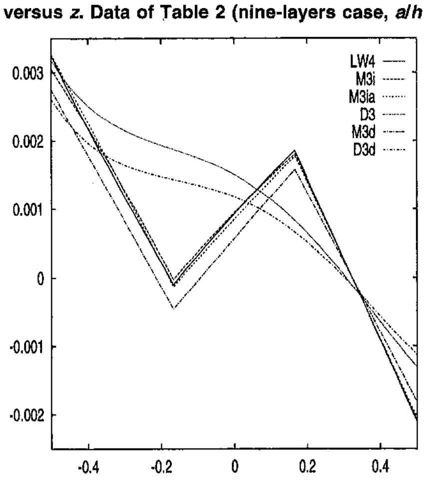

Fig. 9 $\bar{U}_x$ **versus** z**. Square plate made of isotropic layers (Unsymmetrically laminated case,** $a/h = 4$**).**

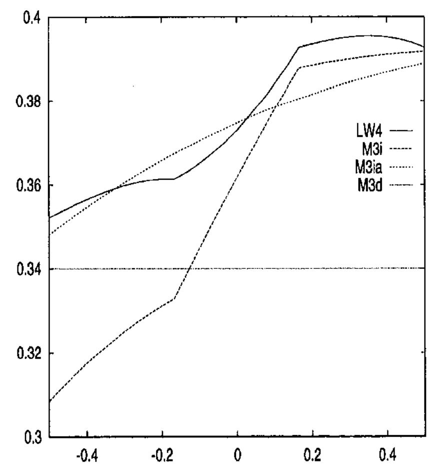

Fig. 11 $\bar{U}_z$ **versus** z**. Square plate made of isotropic layers (Unsymmetrically laminated case,** $a/h = 4$**).**

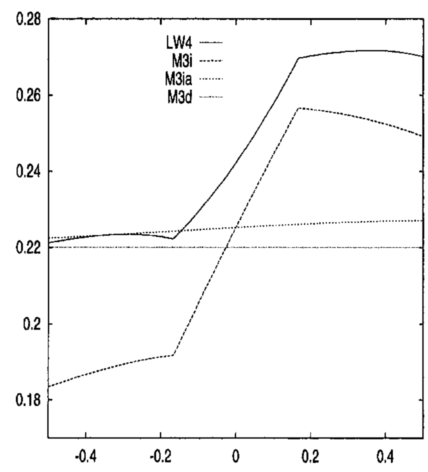

Fig. 12 $\bar{U}_z$ **versus** z**. Square plate made of isotropic layers (Symmetrically laminated case,** $a/h = 4$**).**

tions, related results are depicted by suffix-3D.[1] The superiority has to be registered of modeling including σ_{zz} as well as of referring to the mixed approach with respect to the displacement one. Major differences for the different theories, with respect to those in the previous tables, can be observed in Figs. 5 and 6 where $\bar{U}_z$ versus z has been plotted for a three and a four-layered plate, respectively. It should be noticed that the laminated plates being transversely isotropic (i.e., $E_z = E_T$ does not vary in the thickness direction) the zigzag terms u_{Z_z} of Eq. (8) could introduce an unmotivated constraint. The zigzag form has infact barely been exhibited by the LW4 analysis and better results have been obtained by the M3ia analysis.

The results on the thickness ratio effects are given in Table 4 and Figs. 7 and 8. Unrealistic symmetric distributions of and transverse shear stress discussed in Fig. 3, for those analyses which neglect σ_{zz}, can be confirmed for the case of Fig. 8 and extended to the in-plane displacement diagram of Fig. 7. It should be noticed that the maximum values $(S_{xz}/p_{zt}^{N_l})_{\max} \approx .4 \times 2.5 \approx 1.$ is almost coincident to the maximum σ_{zz} value $(S_{zz}/p_{zt}^{N_l})_{\max} = 1.$ for the thicker plate case: This is the simple reason why σ_{zz} cannot be neglected in thick plate analysis. Symmetry is reached for thinner plates. The superiority of modelings which include σ_{zz} as well as the convenience of referring to mixed descriptions has been confirmed.

A multilayered plate with nonconstant distribution of Young modulus E_z in the thickness direction has been considered in Figs. 9–12. A three-layered thick plate constituted by isotropic ($\nu = .3$) layers has been investigated. Figures 9–11 consider unsymmetrically laminated plates with $E^1/E^2 = 10$; $E^3/E^2 = 100$ where E^k ($k = 1, 2, 3$) are the Young moduli of the three layers. Fig. 12 considers a symmetrically laminated plate $E^1/E^2 = E^3/E^2 = 100$. The E^2 modulus has been used in the considered nondimensioned amplitudes. The superiority of the mixed cases over the displacement ones is evident. Nevertheless, for such a transversely anisotropic plate and in contrast to what has been written for the case of Figs. 5 and 6, the LW4 analysis of Figs. 9 and 12 shows an evident zigzag form for $\bar{U}_z$. Therefore, better results are obtained with the M3i analysis than with the M3ia ones. On the other hand the differences between M3i and LW4 analyses are larger than those experienced for the treated cross-ply plates. Such a conclusion draws attention to the fundamental limitation of two-dimensional modelings which preserve the number of the variables independent from the numbers of layers: They cannot accurately describe σ_{zz} and the related effects of thick structures even though mixed models are implemented. That is, a layer-wise description is required for this purpose.

6 Conclusions

This paper has evaluated the effects of transverse normal stress in two-dimensional modeling of multilayered plates which preserve the number of the unknown variables to be independent from the number of layers. Mixed formulations have been used for this purpose. A comparison with the classical displacement formulation has also been considered. From the conducted investigation the following main remarks can be made.

1 The a priori fulfillment of the interlaminar continuity for σ_{zz} makes mixed models more attractive than other available models which violate such a continuity.
2 Thick plate analysis has shown that refinements of existing theories can be meaningless unless both interlaminar continuous transverse shear and normal stresses are taken into account in a refined theory.
3 The number of the independent variables should be conveniently taken dependent on N_l in very thick plate analysis. Such a requirement becomes mandatory for the case of transversely anisotropic multilayered plates.

The conclusions reached in this paper have been restricted to bended, simply supported orthotropic plates. Additional investigations should be addressed to different geometries, boundary conditions, as well as multilayered lay-outs. Finite element method could be conveniently used to these aims. Works in this direction are in progress and results could be proposed in future works. However, the proposed closed-form results could be used as reference solution to assess approximated analyses.

[1] Even though the mixed models furnish σ_{zz} a priori, its a posteriori evaluation has been preferred for two reasons: (1) to compare consistent results (classical formulation do not permit a priori evaluations); (2) the integration of three-dimensional equilibrium equations leads to better results (Bhaskar and Varadan, 1992; Carrera, 1996).

Acknowledgments

The author is deeply indebted to the late Prof. Eric Reissner for his encouragement to work on the subject of this paper. Further acknowledgments are directed to the late Prof. Placido Cicala for the many suggestions and criticisms given during the review process of the paper (Carrera, 1995).

References

Ambartsumian, S. A., 1968, "On General Theory of Anisotropic Shells," *PMM*, Vol. 22, No. 2, pp. 226–237.

Barbero, E. J., Reddy, J. N., and Teply, J. L., 1990, "General Two-Dimensional Theory of laminated Cylindrical Shells," *American Institute of Aeronautics and Astronautics Journal*, Vol. 28, pp. 544–553.

Bhashar, B., and Varadan, T. K., 1989, "Refinement of Higher-Order Laminated Plate Theories," *American Institute of Aeronautics and Astronautics Journal*, Vol. 27, pp. 1830–1831.

Bhaskar, K., and Varadan, T. K., 1992, "Reissner's New Mixed Variational Principle Applied to Laminated Cylindrical Shells," ASME *Journal of Pressure Vessel Technology*, Vol. 114, pp. 115–119.

Carrera, E., 1995, "A Class of Two Dimensional Theories for Multilayered Plates Analysis," *Atti Accademia delle Scienze di Torino, Mem Sci. Fis.*, Vol. 19–20, pp. 49–87.

Carrera, E., 1996, "C^0 Reissner-Mindlin Multilayered Plate Elements Including Zig-Zag and Interlaminar Stresses Continuity," *International Journal for Numerical Methods in Engineering*, Vol. 39, pp. 1797–1820.

Carrera, E., 1997, "C_z^0-Requirements: Models for the Two-Dimensional Analysis of Multilayered Structures," *Composite Structures*, Vol. 37, pp. 373–383.

Carrera, E., 1998a, "Evaluation of Layer-Wise Mixed Theories for Laminated Plates Analysis," *American Institute of Aeronautics and Astronautics Journal*, Vol. 36, pp. 830–839.

Carrera, E., 1998b, "Layer-Wise Mixed Models for Accurate Vibration Analysis of Multilayered Plates," ASME Journal of Applied Mechanics, Vol. 65, pp. 820–828.

Carrera, E., 1998c, "A Reissner's Mixed Variational Theorem Applied to Vibrational Analysis of Multilayered Shell," ASME Journal of Applied Mechanics, Vol. 66, pp. 69–78.

Cho, K. N., Bert, C. W., and Striz, A. G., 1991, "Free Vibrations of Laminated Rectangular Plates Analyzed by Higher Order Individual-Layer Theory," *Journal of Sound and Vibration*, Vol. 145, pp. 429–442.

Cheung, Y. K., and Wu, C. I., 1972, "Free Vibrations of Thick, Layered Cylinders Having Finite Length With Various Boundary Conditions," *Journal of Sound and Vibration*, Vol. 24, pp. 189–200.

Cho, M., and Parmerter, R. R., 1993, "Efficient Higher Order Composite Plate Theory for General Lamination Configurations," *American Institute of Aeronautics and Astronautics Journal*, Vol. 31, pp. 1299–1305.

Di Sciuva, M., 1993, "A General Quadrilater Multilayered Plate Element With Continuous Interlaminar Stresses," *Composite Structures*, Vol. 47, pp. 91–105.

Grigolyuk, E. I., and Kulikov, G. M., 1988, "General Direction of the Development of the Theory of Shells," *Mekhanica Kompozitnykh Materialov*, No. 2, pp. 287–298.

Hildebrand, F. B., Reissner, E., and Thomas, G. B., 1940, "Notes on the Foundations of the Theory of Small Displacement of Orthotropic Shells," NACA TN-1833, Washington, DC.

Idlbi, A., Karama, M., and Touratier, M., 1997, "Comparison of Various Laminated Plate Theories," *Composite Structures*, Vol. 37, pp. 173–184.

Jing, H., and Tzeng, K., 1993, "Refined Shear Deformation Theory of Laminated Shells," *American Institute of Aeronautics and Astronautics Journal*, Vol. 31, pp. 765–773.

Lekhnitskii, S. G., 1935, "Strength Calculation of Composite Beams," *Vestnik inzhen. i tekhnikov*, No. 9.

Lo, K. H., Christensen, R. M., and Wu, E. M., 1977, "A Higher-Order Theory of Plate Deformation, Part 2: Laminated Plates," ASME Journal of Applied Mechanics, Vol. 44, pp. 669–676.

Murakami, H., 1986, "Laminated Composite Plate Theory With Improved In-Plane Response," ASME Journal of Applied Mechanics, Vol. 53, pp. 661–666.

Noor, A. K., and Burton, W. S., 1989, "Stress and Free Vibration Analyses of Multilayered Composite Plates," *Composite Structures*, Vol. 11, pp. 183–204.

Pagano, N. J., 1969, "Exact Solutions for Composite Laminates in Cylindrical Bending," *Journal of Composite Materials*, Vol. 3, pp. 398–411.

Rath, B. K., and Das, Y. C., 1973, "Vibration of Layered Shells," *Journal of Sound and Vibration*, Vol. 28, pp. 737–757.

Reddy, J. N., 1997, *Mechanics of Laminated Composite Plates, Theory and Analysis*, CRC Press, Boca Raton, FL.

Reissner, E., 1984, "On a Certain Mixed Variational Theory and a Proposed Applications," *International Journal for Numerical Methods in Engineering*, Vol. 20, pp. 1366–1368.

Reissner, E., 1985, "Reflections on the Theory of Elastic Plates," Applied Mechanics Review, Vol. 38, pp. 1433–1464.

Reissner, E., 1986, "On a Mixed Variational Theorem and on a Shear Deformable Plate Theory," *International Journal for Numerical Methods in Engineering*, Vol. 23, pp. 193–198.

Ren, J. G., 1986, "A New Theory for Laminated Plates," *Composite Science and Technology*, Vol. 26, pp. 225–239.

Ren, J. G., 1987, "Exact Solutions for Laminated Cylindrical Shells in Cylindrical Bending," *Composite Science and Technology*, Vol. 29, pp. 169–187.

Robbins, D. H., Jr., and Reddy, J. N., 1993, "Modeling of Thick Composites Using a Layer-Wise Theory," *International Journal of Numerical Methods in Engineering*, Vol. 36, pp. 655–677.

Soldatos, K. P., and Timarci, T., 1993, "A Unified Formulation of Laminated Composites, Shear Deformable, Five-Degrees-of-Freedom Cylindrical Shell Theories," *Composite Structures*, Vol. 25, pp. 165–171.

Srinivas, S., 1973, "A Refined Analysis of Composite Laminates," *Journal of Sound and Vibration*, Vol. 30, pp. 495–50.

Szabo, B., and Sahrmann, A., 1988, "Hierarchic Plate and Shell Models Based on p-Extension," *International Journal for Numerical Methods in Engineering*, Vol. 8, pp. 495–450.

Surana, S. K., and Sorem, R. M., 1991, "Completely Hierarchical p-Version Curved Shell Elements for Laminated Composite Plates and Shells," *Computational Mechanics*, pp. 237–251.

Toledano, A., and Murakami, H., 1987a, "A Composite Plate Theory for Arbitrary Laminated Configurations," ASME Journal of Applied Mechanics, Vol. 54, pp. 181–189.

Toledano, A., and Murakami, H., 1987b, "A Higher-Order Laminated Plate Theory with Improved In-Plane Responses," *International Journal of Solids and Structures*, Vol. 23, pp. 111–131.

Varadan, T. K., and Bhaskar, K., 1991, "Bending of Laminated Orthotropic Cylindrical Shells—An Elasticity Approach," *Composite Structures*, Vol. 17, pp. 141–156.

Whitney, J. M., 1969, "The Effects of Transverse Shear Deformation on the Bending of Laminated Plates," *Journal of Composite Materials*, Vol. 3, pp. 534–547.